THE IMPROVED TAIWAN IONOSPHERIC MODEL (TWIM) AND ITS APPLICATIONS ON GPS POSITIONING

L.-C. Tsai[a, b], C. W. Zheng[b], Ernest P. Macalalad[b], G. H. Chen[c], and M. H. Tien[d]

[a] Center for Space and Remote Sensing Research, National Central University (NCU), Chung-Li, Taiwan; lctsai@csrsr.ncu.edu.tw

[b] Graduate Institute of Space Science, NCU, Chung-Li, Taiwan

[c] Multimedia and Game Science Department, Taipei College of Maritime Technology (TCMT), Taipei, Taiwan

[d] Department of Marine Leisure and Tourism, TCMT, Taipei, Taiwan

KEY WORDS: Ionospheric electron density model, GPS radio occultation, GPS positioning

Abstract: A three-dimensional ionospheric electron density (*Ne*) model (L.-C. Tsai, C. H. Liu, T. Y. Hsiao, and J. Y. Huang, Radio Sci., 44, doi:10.1029/2009RS004154, 2009) has been named the TaiWan Ionospheric Model (TWIM) and constructed from vertical *Ne* profiles retrieved from FormoSat3/COSMIC GPS radio occultation measurements. We further improved the TWIM by including global distributed ionosonde *foF2* and *foE* data and qualifying COSMIC *Ne* profiles based on the empirical orthogonal function (EOF) classification. The improved TWIM also exhibits vertically-fitted α-Chapman-type layers, with distinct F2, F1, E, and D layers, and surface spherical harmonics approaches for the fitted layer parameters including peak density, peak density height, and scale height. These results are useful in investigation of near-Earth space and large-scale *Ne* distribution. This way the continuity of *Ne* and its derivatives is also maintained for practical schemes for providing reliable radio propagation predictions. We have presented a numerical and step by step ray-tracing method (L.-C. Tsai, C. H. Liu, and J. Y. Huang, Radio Sci., 45, doi:10.1029/2010RS004359, 2010) on the TWIM and including an Earth-centered magnetic dipole and horizontal *Ne* gradient effects. The ray-tracing methodology has potential applicability to ionospheric correction as applied to GPS positioning. In this paper, ionospheric corrections on both single-receiver and double-receiver L1 GPS code measurements using the TWIM have been presented and evaluated. Its performances with respect with the ionospheric corrections using other ionospheric models are also presented and compared.

SPACED-BASED GPS RADIO OCCULTATION OBSERVATIONS AND THE TAIWAN IONOSPHERIC MODEL (TWIM)

The TWIM is constructed from the Taiwan FormoSat3 / Constellation Observing

System for Meteorology, Ionosphere and Climate (FS3/COSMIC) data mostly. The FS3/COSMIC program includes six spacecraft (FM1 to FM6) located at a nearly circular orbit of ~800 km altitude, ~70° inclination angle, and 60° separation to receive GPS signals. The Global Positioning System (GPS) radio occultation (RO) technique has been used to receive multi-channel GPS carrier phase signals at low Earth orbiting (LEO) satellites performing active limb sounding of the Earth's atmosphere and ionosphere. Generally FS3/COSMIC can obtain over 2500 RO measurements per day, providing data for the atmosphere and ionosphere including areas over the oceans, the southern hemisphere, where few ground-based stations are located. For further details about the FS3/COSMIC program, see [*Rocken et al.*, 2000; *Hajj et al.*, 2000]. Each GPS RO observation consists of a set of limb-viewing links with tangent points ranging from the LEO satellite orbit altitude to the Earth's surface. The path TEC values are obtained from differential GPS phase measurements using both the L1 and L2 radio signals. The N_e values can be retrieved from the calibrated or compensated TEC values [*Schreiner et al.*, 1999; *Tsai et al.*, 2009a] using the Abel integral transform given by *Tricomi* [1985] defined as:

$$N_e(r_t) = -\frac{1}{\pi}\int_{r_t}^{r_{LEO}} \frac{d\,TEC(r)/dr}{\sqrt{r^2 - r_t^2}}\,dr\,. \qquad (1)$$

The N_e value at a tangent point's radial distance r_t can be computed in a recursive way starting from the outmost ray at r_{LEO} and its N_e profile can then be obtained to the base of the ionosphere.

The terrestrial ionosphere at all latitudes has a tendency to separate into layers at different altitude regions. Specifically, the N_e profiles exhibit layered structures, with distinct F2, F1, E, and D layers, despite the fact that different physical processes dominate in different latitudinal region. In the TWIM each layer is generally characterized by a Chapman-type function described by the parameters of peak N_e (N_{emax}), peak density height (h_m), and scale height (H), and the layer parameters can be obtained with least-squares error fitting of the observed profile to the Chapman functions.

$$N_e(\theta,\lambda,h) = \sum_{i=1}^{4} N_{e\max}^{i}(\theta,\lambda)\cdot e^{\frac{1}{2}\left(1-\frac{h-h_m^i(\theta,\lambda)}{H^i(\theta,\lambda)}-e^{-\frac{h-h_m^i(\theta,\lambda)}{H^i(\theta,\lambda)}}\right)} \qquad (2)$$

where each i means a physical layer of F2, F1, E, or D layer. A Chapman-type layer is predicted by a simplified aeronomic theory, assuming photoionization in a one-species neutral gas, and neglecting transport processes. All of the layers are usually present during the daytime. The F1 and D layers decay at night and could be hidden within the other layers, but the F1- and D-layer parameters are still derivable throughout all times by least-squares error fitting. In the TWIM a two-dimensional (latitude and longitude) numerical map to fit

derived layer peak N_e, peak density height, or scale height values can be represented by a function $\Gamma(\theta, \lambda)$ and constructed by spherical harmonic analysis of the Laplace's partial differential equation. The resulting real functions of θ (latitude) and λ (longitude or the local time angle) are combinations of the surface spherical harmonics [*Davis*, 1989] defined by

$$\Gamma(\theta,\lambda) = \sum_{m=0}^{3}\sum_{n=0}^{q_m}\left[A_{nm}\, U_{nm}(\theta,\lambda) + B_{nm}\, V_{nm}(\theta,\lambda)\right], \text{where}$$

$$U_{nm}(\theta,\lambda) = \sqrt{\frac{2n+1}{2\pi}\frac{(n-m)!}{(n+m)!}}\, P_n^m(\cos\theta)\cos m\lambda \ , and$$

$$V_{nm}(\theta,\lambda) = \sqrt{\frac{2n+1}{2\pi}\frac{(n-m)!}{(n+m)!}}\, P_n^m(\cos\theta)\sin m\lambda \qquad (3)$$

$$(n = 0, 1, 2, \cdots q_m \ ; m = 0, 1, 2, or\ 3) \ ,$$

and $P_n^m( )$ is the familiar associated Legendre polynomial of the first kind of degree n and order m. After the optimization analyses of noise separation we determined the cutoffs to be an order of 3 and a degree of 20 for each order. For details concerning the performance and evaluation of the TWIM, the interested readers are referred to *Tsai et al.* [2009b]. The three spherical components of N_e gradients are given by

$$\frac{\partial N_e}{\partial h} = \sum_{i=1}^{4} N_{e\max}^i \cdot e^{\frac{1}{2}\left(1-x_i-e^{-x_i}\right)} \cdot \left(-\frac{1}{2}+\frac{1}{2}e^{-x_i}\right)\cdot H^i \ ,$$

$$\frac{1}{r}\frac{\partial N_e}{\partial \theta} = \frac{1}{r}\cdot\left[\begin{array}{l}\sum_{i=1}^{4} e^{\frac{1}{2}\left(1-x_i-e^{-x_i}\right)}\cdot\frac{\partial N_{e\max}^i}{\partial\theta} + \\ \sum_{i=1}^{4} N_{e\max}^i \cdot e^{\frac{1}{2}\left(1-x_i-e^{-x_i}\right)}\cdot\left(-\frac{1}{2}+\frac{1}{2}e^{-x_i}\right)\cdot\left(-\frac{1}{H^i}\frac{\partial h_m^i}{\partial\theta} - \frac{h-h_m^i}{H^{i2}}\frac{\partial H^i}{\partial\theta}\right)\end{array}\right]$$

$$\frac{1}{r\sin\theta}\frac{\partial N_e}{\partial \phi} = \frac{1}{r\sin\theta}\cdot\left[\begin{array}{l}\sum_{i=1}^{4} e^{\frac{1}{2}\left(1-x_i-e^{-x_i}\right)}\cdot\frac{\partial N_{e\max}^i}{\partial\phi} + \\ \sum_{i=1}^{4} N_{e\max}^i \cdot e^{\frac{1}{2}\left(1-x_i-e^{-x_i}\right)}\cdot\left(-\frac{1}{2}+\frac{1}{2}e^{-x_i}\right)\cdot\left(-\frac{1}{H^i}\frac{\partial h_m^i}{\partial\phi} - \frac{h-h_m^i}{H^{i2}}\frac{\partial H^i}{\partial\phi}\right)\end{array}\right], \qquad (4)$$

where $x_i = (h-h_m^i)/H^i$, and i means one of the F2, F1, E, and D physical layers. The phenomenological ionospheric model thus provides temporal and synoptic variations in three-dimensional (latitude, longitude, and altitude) N_e and maintains the continuity in the first and second N_e derivatives for providing reliable radio propagation predictions and electrostatic field determinations.

GPS IONOSPHERIC CORRECTION BY TWIM

This section demonstrates the performance of TWIM in GPS positioning. The results, which

include the total electron content maps, the horizontal and vertical positional errors and RMS values, are compared to the Klobuchar and GIM models at different elevation angles, time, and geographical locations. The percent occurrence of the days that yielded lowest errors for all days of observations is also presented. Nine global VTEC maps for Klobuchar, GIM, and TWIM at epochs 0300UT, 0400UT, and 0500UT on August 22, 2010 (DOY 234) are shown in Fig. 1, which is chosen arbitrarily. The test sites are shown in triangles. The basic diurnal and geographic features of the ionosphere are shown in all nine maps, that is, peak density during day time and in the low-latitude regions while the minimum density is featured during night time and in the mid-latitude regions. We can also observe the westward shift of the peak density area as the time moves forward. The maximum VTEC value shown on the GIM maps is the greatest amongthe three models while the Klobuchar maps displayed the least peak density that is shifted to higher latitudes. The TWIM, on the other hand, provides a more detailed VTEC maps as compared with the other two models. For example, the well-known equatorial ionization anomaly (EIA) is clearly shown in the TWIM VTEC maps in the daytime sector. Furthermore, the TWIM can provide three-dimensional electron densities while Klobuchar and GIM only provide two-dimensional (longitudinal and latitudinal) VTEC models. The calculated 24-h ionospheric slant delays in meters using Klobuchar, GIM, and TWIM on DOY 234 for the three test sites are shown in Fig. 2. The white and gray areas indicate local daytime (0600–1800LT) and nighttime (1800–0600LT). The figure clearly shows the typical diurnal variation of ionosphere where electron density is higher during daytime than in night time. Moreover, the mid-latitude stations (BOR1 and IRKJ) produce low ionospheric delay while the low-latitude station (TWTF) provides high ionospheric slant delays during daytime. This corresponds to the high density provided by the EIA. Meanwhile, all stations yield approximately equal ionospheric slant delays during nighttime. Slant delays calculated from the Klobuchar model are consistent for all stations, showing the half cosine-shaped daytime and constant nighttime electron densities. The GIM-derived slant delays, on the other hand, are closer to the TWIMderived slant delays with the TWIM providing a wider range of values than GIM. However, GIM produce larger ionospheric delay than TWIM. This is because GIM have the largest peak electron density as previously described in Fig. 1. Figure 3 that shows the horizontal errors D and the vertical errors using the three models KLB, GIM, and TWIM for the three stations and epochs 0300UT, 0400UT, and 0500UT for DOY 234. As shown in this figure, the TWIM generally provides the smallest error for the stations in both horizontal and vertical direction. Meanwhile, Klobuchar provide largest error in both horizontal and vertical directions. This indirectly shows that TWIM generally provides a better estimation of the slant TEC around the GPS receivers.

REFERENCES

Davis, Harry F. (1989), *Fourier series and orthogonal functions*, Dover Publications, Inc.,

New York.

Hajj, G. A., L. C. Lee, X. Pi, L. J. Romans, W. S. Schreiner, P. R. Straus, and C. Wang (2000), COSMIC GPS ionospheric sensing and space weather, *Terrestial, Atmospheric and Oceanic Sciences*, 11(1), 235-272.

Rocken, Christian, Y.-H. Kuo, W. Schreiner, D. Hunt, S. Sokolovskiy, and C. McCormick (2000), COSMIC system description, *Terrestial, Atmospheric and* Oceanic Sciences, 11(1), 21-52.

Schreiner, W. S., S. V. Sokolovskiy, C. Rocken, and D. C. Hunt (1999), Analysis and validation of GPS/MET radio occultation data in the ionosphere, *Radio Sci.*, *34(4)*, 949-966.

Tricomi, F. G. (1985), *Integral Equations*, 238 pages, Dover, Mineola, New York.

Tsai, L.-C., C. H. Liu, and T. Y. Hsiao (2009a), Profiling of ionospheric electron density based on the FormoSat-3/COSMIC data: results from the intense observation period experiment, *Terrestial, Atmospheric and Oceanic Sciences*, 20 *(1)*, 181-191, doi: 10.3319/TAO.2007.12.19.01 (F3C).

Tsai, L.-C., C. H. Liu, T. Y. Hsiao, and J. Y. Huang (2009b), A near real-time phenomenological model of ionospheric electron density based on GPS radio occultation data, *Radio Sci.*, *44*, doi:10.1029/2009RS004154.

Tsai, L.-C., C. H. Liu, and J. Y. Huang (2010), Three-dimensional and numerical ray tracing on a phenomenological ionospheric model, *Radio Science* (SCI Journal), 45, doi:10.1029/2010RS004359.

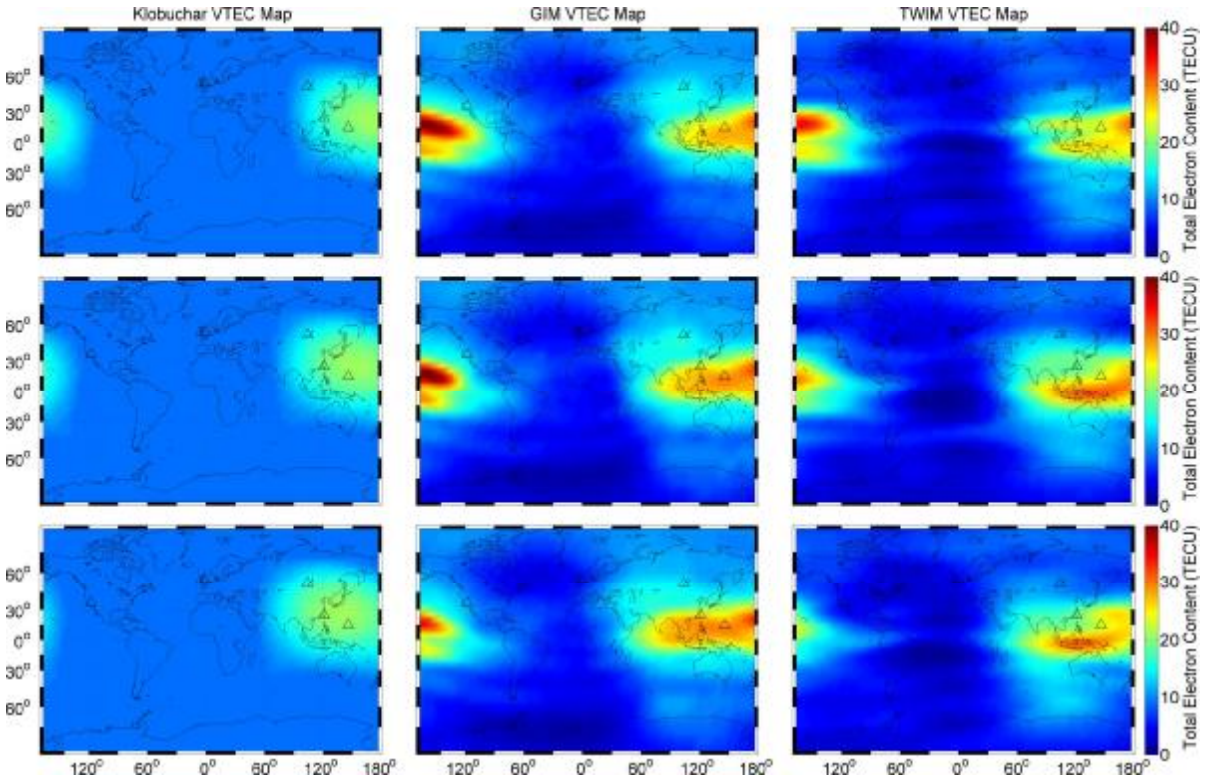

Fig. 1 Global VTEC maps for Klobuchar (col 1), GIM (col 2), and TWIM (col 3) at epochs 0300UT (row 1), 0400UT (row 2) and 0500UT (row 3) for DOY 234

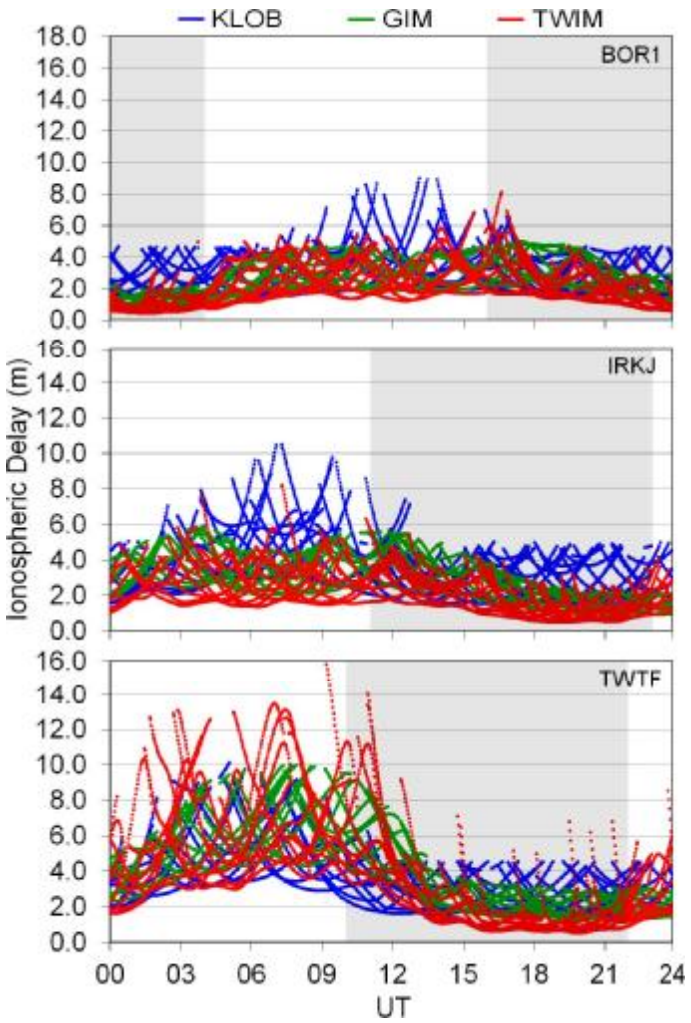

Fig. 2 Slant Ionospheric delay calculated by Klobuchar (KLB), GIM and TWIM for BOR1 (row 1), IRKJ (row 2), and TWTF (row 3) stations for DOY 234

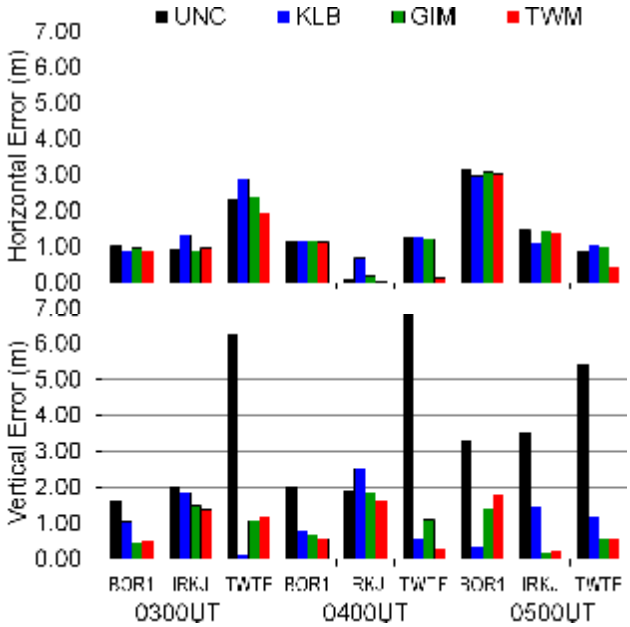

Fig 3 Horizontal (row 1) and vertical (row 2) errors at epochs 0300UT, 0400UT, and 0500UT for DOY 234 for different ionospheric models